JOURNAL OF GUIDANCE, CONTROL, AND DYNAMICS
Vol. 23, No. 4, July–August 2000

Decentralized State Estimation for Flexible Space Structures

Gregory J. W. Mallory* and David W. Miller†
Massachusetts Institute of Technology, Cambridge, Massachusetts 02139

The application of decentralized state estimation for a large-scale system is detailed. Decentralized estimation requires the global system to be decomposed into a set of local models. The local models can have an order less than the global model if uncoupled and weakly coupled dynamics are neglected. Each local model computes a local state estimate, which can be combined to form the global state estimate. A technique is presented, based on model reduction theory, which provides a procedure for generating the local models from a heavily coupled global model. A technique to evaluate the global estimates of a local estimator is derived. A detailed example is presented with the design of a decentralized state estimator for the Space Interferometry Mission (SIM) spacecraft, and the advantages of a global control for SIM are noted. Further, the work provides a technique for quantifying the use of individual sensors for measuring global space-structure modes.

I. Introduction

THE conventional control strategy for a large flexible spacecraft is a decentralized approach.[1] In the control design for a space telescope, the rigid-body attitude control is decoupled from the higher bandwidth optical control. Typically, the optical control is further decoupled into high-frequency and low-frequency control loops. Each decoupled, local, control loop is designed separately by ignoring coupling with other loops, and the control loops are closed sequentially. Research is underway to understand the limitations of the decentralized approach and to investigate the possible advantages of a global control design.[2] Further, investigating the estimate quality achieved by local estimators can provide the designer with information of the suitability of a system's sensor suite for local estimation and control. In this paper decentralization of the state estimation part of the control problem is studied. The contribution of the paper is the complete development of a decentralized state estimator including 1) a method for recovering the optimal global estimate from a set of local estimators, 2) a method for determining the order of the local models, 3) an analysis technique to quantify the accuracy penalty of using local models, and 4) a validation example on a complex system.

It is well known from estimation theory that, given a linear system and the correct system model, a Kalman filter provides the state estimate, which minimizes the rms error. This global Kalman filter must use the full-state system model, and it must have access to the noisy measurements from all sensors. In certain large-scale systems the high order of the system and the large number of sensors can make the traditional global estimator intractable. Complete communication of all sensor information can be expensive. The problem is further compounded by geographically separated sensors, as in, for example, a power network or multiple scanning sensors in a multiple-target radar tracking problem. The high system order and strict requirements on sensor communication favor a decentralized estimation approach.

Decentralized estimation involves estimating the state at each sensor node. Each node is assumed to have an associated local model and a processor. The ith node estimate is updated from measurements only generated at the ith node. Decentralized estimation and its dual, decentralized control, have long been a subject of research for large-scale systems.[3] A detailed survey of early work in decentralized control is provided in Ref. 4. When the global system is cast into a set of local systems for decentralized estimation, the designer must ensure that the neglected coupling (interaction) terms between the local models do not destabilize the local estimator (designed stable on the local model). The decentralized estimator in Ref. 3, and more recently in Refs. 5 and 6, ensure stability for special classes of systems, but optimality is not necessarily preserved. Optimality in this context can be defined as the ability to combine the local state estimates and error covariances in a way such that the optimal state estimate of the global Kalman filter is recovered.

The work of Ref. 7 derives a parallel Kalman-filter structure, which does preserve optimality. Each sensor node is equipped with the full-order model of the system dynamics, and all nodes intercommunicate. In this manner the global estimate is obtained at each node. This work was generalized in Ref. 8 to local models satisfying a dynamics exactness condition. Similar work, based on the information form of the Kalman filter, is developed in Ref. 9 for the full-order decentralized information filter and Refs. 10–12 for a reduced-order local model case. Generally, the lower-order model is fully coupled, although some modes may be unobservable, or only slightly observable to the ith sensor. In this paper a method to extract the local models from the global model based on state observability is developed.

The paper is divided as follows. A decentralized estimator is presented in Sec. II. The chosen estimator maintains the ability to combine local estimates into an optimal global estimate should internode communication be allowed. In Sec. III, a method for extracting local models from the global system is presented. Section IV culminates the work by applying the decentralized estimation scheme to a very complex, large-scale system, the model for the Space Interferometry Mission (SIM) spacecraft.

II. Decentralized Estimator

In this section we present the decentralized estimator as developed in Ref. 11 and refined in Ref. 12, generalized for the time-variant case. Consider an nth order discrete-time global model, disturbed by p process noises, and measured by m sensors:

$$x(k+1) = A(k)x(k) + L(k)w(k) \tag{1}$$

$$z(k) = C(k)x(k) + v(k) \tag{2}$$

where, $x_0 \sim N(\bar{x}_0, P_0)$ is a normal white-noise process of mean $\bar{x}_0$ and symmetric, positive definite covariance P_0. Similarly, $w(k) \sim N[0, \Xi(k)]$ is the process noise, and $v(k) \sim N[0, \Theta(k)]$ is the sensor noise. $w(k)$ and $v(k)$ are assumed independent from each other and from the initial condition x_0. $x(k) \in \Re^n$, $w(k) \in \Re^p$, $v(k) \in \Re^m$, $A(k) \in \Re^{n \times n}$, $L(k) \in \Re^{n \times p}$, and $C(k) \in \Re^{m \times n}$. In this paper all development and simulation will be for the discrete-time filter to preserve the decoupling of the traditional predict and update cycles.

Received 22 April 1999; revision received 7 December 1999; accepted for publication 14 December 1999.

*Graduate Research Assistant, Space Systems Laboratory. Student Member AIAA.
†Assistant Professor, Director, Space Systems Laboratory. Member AIAA.

A. Centralized State Estimators

We begin the development of the decentralized estimator by reviewing two forms of the global (centralized) state estimator. Given this model, the discrete Kalman filter[13] is generated by

$$\hat{x}(k+1\,|\,k) = A(k)\hat{x}(k) \tag{3}$$

$$P_m = A(k)P(k)A^T(k) + L(k)\Xi(k)L^T(k) \tag{4}$$

forming the predict cycle, and

$$\hat{x}(k+1) = \hat{x}(k+1\,|\,k) + K(k+1)[z(k+1) - C(k+1)\hat{x}(k+1\,|\,k)] \tag{5}$$

$$\begin{aligned} P(k+1) &= [I - K(k+1)C(k+1)]P_m \\ &= P_m - P_m C(k+1)[C(k+1)P_m C^T(k+1) \\ &\quad + \Theta(k+1)]^{-1} C(k+1)P_m \end{aligned} \tag{6}$$

$$\begin{aligned} K(k+1) &= P(k+1)C^T(k+1)\Theta^{-1}(k+1) \\ &= P_m C^T(k+1)[C(k+1)P_m C^T(k+1) + \Theta(k+1)]^{-1} \end{aligned} \tag{7}$$

forming the measurement update cycle. In the preceding relations we dropped the index of the $k+1$ predict cycle state estimate error covariance $P_m = P(k+1\,|\,k)$.

By transforming to information variables, the information matrix $Y(i\,|\,j) = P^{-1}(i\,|\,j)$ and the information state $y(i\,|\,j) = Y(i\,|\,j)x(i\,|\,j)$, the Kalman filter can be rewritten as an information filter with

$$\hat{y}(k+1\,|\,k) = Y_m A(k)Y(k)\hat{y}(k) \tag{8}$$

$$Y_m = [A(k)Y(k)^{-1}A^T(k) + L(k)\Xi(k)L^T(k)]^{-1} \tag{9}$$

forming the predict cycle, and

$$\hat{y}(k+1) = \hat{y}(k+1\,|\,k) + C^T(k+1)\Theta^{-1}(k+1)z(k+1) \tag{10}$$

$$Y(k+1) = Y_m + C^T(k+1)\Theta(k+1)C(k+1) \tag{11}$$

forming the update cycle. The information filter is derived and shown to be algebraically equivalent to the Kalman filter in the Appendix. We see that the information filter has a much simpler (from a computational point of view) update cycle than the traditional Kalman filter, but suffers from a more complex predict cycle.

B. Decentralizing the Filter

We will present a decentralized filter, which is a hybrid of the Kalman and information filters, derived from combining two filters presented in Ref. 12. Consider the measurement vector $z = [z_1 \;\; z_2 \;\; \cdots \;\; z_q]^T$, where we have partitioned the vector into a column of single sensor measurements. The development holds equally for multiple sensor partitions. The output equation is thus partitioned as $C = [C_1^T \;\; C_2^T \;\; \cdots \;\; C_q^T]^T$ and the sensor noise as $v = [v_1 \;\; v_2 \;\; \cdots \;\; v_q]^T$. We make the assumption that each sensor has an independent noise process, and thus the sensor noise covariance can be decoupled as $\Theta = \text{diag}\{\Theta_1, \Theta_2, \ldots, \Theta_q\}$.

The assumption of independent sensor noises allows us to decentralize the update (measurement) cycle of the Kalman filter while maintaining local estimates, which can be globally recombined into the optimal state estimates. The assumption of independent sensor noise is valid if the sensors indeed generate their own noise, in the form of quantization error for example, but does not hold if the sensor noise is generated by some underlying process. An example where the independent sensor noise assumption is not valid is in the case where radar sensors are being jammed. The challenging decentralized estimation problem in the presence of correlated sensor noises is studied in Ref. 14.

Now, assume that the ith local model exists, corresponding to the z_i measurement. The model is given by

$$x_i(k+1) = A_i(k)x_i(k) + L_i(k)w(k) \tag{12}$$

$$z_i(k) = c_i(k)x_i(k) + v_i(k) \tag{13}$$

with $x_i(k) \in \Re^{n_i}$, $A_i(k) \in \Re^{n_i \times n_i}$, $L_i(k) \in \Re^{n_i \times p}$, and $c_i(k) \in \Re^{1 \times n_i}$. For the local model to be exact, we must have

$$C_i(k)x(k) = c_i(k)x_i(k) \tag{14}$$

which is a type of dynamics exactness relation.[4]

At the ith local node we implement an optimal local filter, combining elements of the Kalman and information filters, resulting in a predict cycle given by

$$\hat{x}_i(k+1\,|\,k) = A_i(k)\hat{x}_i(k) \tag{15}$$

$$P_{mi}(k+1) = A_i(k)P_i(k)A_i^T(k) + L_i(k)\Xi(k)L_i^T(k) \tag{16}$$

The local measurement update cycle can be written in information form as

$$\hat{y}_i(k+1) = \hat{y}_i(k+1\,|\,k) + c_i^T(k+1)\Theta_i^{-1}(k+1)z_i(k+1) \tag{17}$$

$$Y_i(k+1) = Y_{mi} + c_i^T(k+1)\Theta_i(k+1)c_i(k+1) \tag{18}$$

where we have substituted our appropriate ith local model parameters into the global optimal filter. Recall the information matrices and covariance matrices are related by $Y(k) = P^{-1}(k)$ and $Y_{mi}(k) = P_{mi}^{-1}(k)$.

We have written the local estimator for each sensor node. We wish to develop an estimator (the decentralized estimator) that can recover the optimal global Kalman-filter estimate from the local estimates. With our partition of the measurements, we can rewrite Eq. (10) for the global information update as

$$\begin{aligned} \hat{y}(k+1) &= \hat{y}(k+1\,|\,k) + \begin{bmatrix} C_1^T & \cdots & C_m^T \end{bmatrix} \\ &\quad \times \text{diag}\left\{\Theta_1^{-1}, \ldots, \Theta_m^{-1}\right\}[z_1 \quad \cdots \quad z_m]^T = \hat{y}(k+1\,|\,k) \\ &\quad + \sum_{i=1}^{m} C_i^T(k+1)\Theta_i^{-1}(k+1)z_i(k+1) \end{aligned} \tag{19}$$

We choose a transformation $T_{ci}(k)$ such that the following relation holds between the ith global output vector C_i and the ith local output vector c_i:

$$C_i(k) = c_i(k)T_{ci}(k) \tag{20}$$

The exact choice of $T_{ci}(k)$ will be based on model reduction and will be detailed in Sec. III. In general though, if the local and global state are related through the transformation $x_i(k) = T_i(k)x(k)$ and the transformation has a unique pseudoinverse (Moore–Penrose generalized inverse[15]) $T_i^\dagger$, then by using Eq. (14) we have $T_{ci}(k) = T_i(k)$. If the state transformation does not have a unique pseudoinverse, then we can often use $T_{ci}(k) = c_i^\dagger(k)C_i(k)$, where the right pseudoinverse of c_i has been used. Because we have decoupled single sensors, such that C_i has full row rank, then we can always find a relation T_{ci} such that Eq. (20) holds.

Substituting Eq. (20) into Eq. (19), we have

$$\hat{y}(k+1) = \hat{y}(k+1\,|\,k) + \sum_{i=1}^{m} T_{ci}^T(k+1)c_i^T(k+1)\Theta_i^{-1}(k+1)z_i(k+1) \tag{21}$$

Substituting Eq. (17) results in

$$\hat{y}(k+1) = \hat{y}(k+1\,|\,k) + \sum_{i=1}^{m} T_{ci}^T(k+1)[\hat{y}_i(k+1) - \hat{y}_i(k+1\,|\,k)] \tag{22}$$

a decentralized version of Eq. (10). Using a similar approach, we can write Eq. (11) as

$$\begin{aligned} Y(k+1) &= Y_m + \sum_{i=1}^{m} C_i^T(k+1)\Theta_i(k+1)C_i(k+1) \\ &= Y_m + \sum_{i=1}^{m} T_{ci}^T(k+1)c_i^T(k+1)\Theta_i(k+1)c_i(k+1)T_{ci}(k+1) \end{aligned} \tag{23}$$

which, when we substitute Eq. (18), results in

$$Y(k+1) = Y_m(k+1) + \sum_{i=1}^{m} T_{ci}^T(k+1)[Y_i(k+1) - Y_{mi}(k+1)]T_{ci}(k+1) \tag{24}$$

Equations (22) and (24) are decentralized measurement update equations in information form. This filter preserves the optimality of the global estimator. To recover the decentralized measurement update equations in conventional notation, it is a matter of substituting conventional states and covariance matrices for the information state and the information matrices, respectively. Compared with other techniques, this decentralized filter sacrifices local estimate performance, to allow the recovery of the optimal global estimate.

Each local Kalman filter must pass two information state variables $\hat{y}_i(k+1)$ and $\hat{y}_i(k+1\,|\,k)$, both of size $n_i \times 1$, as well as two information matrices $Y_i(k+1)$ and $Y_{mi}(k+1)$, both of size $n_i \times n_i$. Symmetry of the information matrix requires that only a triangular partition be passed. If the filter is implemented with conventional variables, we must pass the corresponding system state and covariance matrices. This filter is advantageous because it passes data one way from the local estimators to the fusion center.

The filter is only partially decentralized. The local estimates are recombined in the measurement update cycle, but the predict cycle still requires the use of Eqs. (3) and (4). In the special case where 1) the process noise decouples in an analogous way to the measurement noise, i.e., $\Xi = \text{diag}\{\Xi_1, \Xi_2, \ldots, \Xi_m\}$, then 2) we have

$$x_i(k+1) = A_i(k)x_i(k) + L_i(k)w_i(k) \tag{25}$$

and 3) local process noises w_i are independent, then further decentralization of the time update equation can be achieved.[12] However, decoupling the process noise is not a valid assumption in the applications explored in this paper. For example, the reaction wheels of SIM are the primary disturbance sources, and their effect can be observed by all system sensors. Thus when local models are formed, the individual process noises are strongly correlated.

As shown in Fig. 1, as long as we choose our local models such that Eq. (20) is satisfied, then through Eqs. (22) and (24) we maintain a way to combine the local estimates into an optimal global estimate.

At each sensor node the developed estimator allows us to obtain a local estimate of the state, which could be used by a local controller. If the global estimate is required, one-way communication from the sensor nodes to the central estimator allows recovery of the optimal global estimate.

By computing the number of multiplications at each time step, the traditional Kalman filter and the developed decentralized filter can be compared in terms of computational complexity. Following the development of Ref. 16, the number of computations per cycle for both methods can be compared. The decentralized filter requires more total computations because local estimates must be computed along with the global estimate. If we assume the local estimates are computed on parallel processors, then most multiplications take place at the estimation fusion processor. For a standard implementation the decentralized central processor requires marginally more computations than the global optimal filter. Other computation algorithms exist (e.g., square-root methods), and thus numerical complexity is more a function of implementation than of method.

The decentralized filter increases our tolerance to sensors failure[10] and our ability to detect and isolate faults.[17]

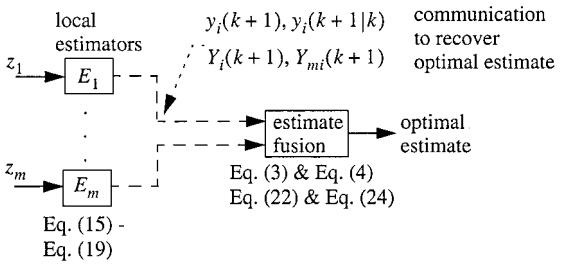

Fig. 1 Recovering optimal estimates from local estimates.

III. Local Model Selection

We now develop a technique for selecting local models. The technique is founded on model reduction. The local models are not optimal but are selected using a sound engineering method, which we will later demonstrate applies to large-scale physical systems, in particular flexible space structures. One technique uses physical coordinates for selecting reduced-order models for decentralized estimation.[10] A problem with this method is that large-scale systems are rarely described by physical models. They are typically described with a reduced-order finite element method (FEM). Other techniques, such as ε decomposition to extract local dynamics based on the size of elements of the A matrix, are plagued with similar difficulties.[18,19] We present an alternate technique.

A. Local Balanced Truncation

By examining the dynamics of Eqs. (1) and (2), we conclude that coupling can be achieved through four mechanisms: 1) mechanical coupling through the structure (non-block-diagonal A), 2) measurement coupling through sensors (C), 3) disturbance input matrix coupling (L), and 4) sensor noise coupling through nondiagonal sensor noise covariance (Θ). We need not consider coupling through the positive semidefinite process noise covariance because it can be transformed as $\Xi = U\Lambda U^T$ with diagonal Λ so that we can write $\underline{L} = LU\Lambda^{1/2}$ with a transformed uncorrelated process noise covariance $\underline{\Xi} = I$. Thus, process noise correlation has an analogous effect as L matrix coupling. We make an assumption that the first three sources of coupling are dominant and that sensors have independent sensor noise.

Consider a full-order model at the ith sensor node. This model has Eq. (1) as a state equation and

$$z_i(k) = C_i x(k) + n_i(k) \tag{26}$$

as the measurement equation. For stable, linear time-invariant (LTI) discrete systems the controllability grammian satisfies the following discrete-time Lyapunov equation:

$$W_c = AW_cA^T + LL^T \tag{27}$$

which provides a relative measure of the controllability of the states from the process noise. The larger the jth diagonal of W_c (relative to other diagonals), the more controllable the jth state will be (relative to other states). In a dual sense the observability grammian for our full-order model satisfies

$$W_o = A^T W_o A + C_i^T C_i \tag{28}$$

where the diagonals of W_o correspond to measures of relative observability for the ith sensor.

Consider a general state transformation of the form $\underline{x} = Tx$. By substituting into Eqs. (1) and (2), a transformed state space system can be obtained:

$$\underline{x}(k+1) = \underline{A}\underline{x}(k) + \underline{L}w(k) \tag{29}$$

$$z(k) = \underline{C}\underline{x}(k) + v(k) \tag{30}$$

with $\underline{A} = TAT^{\dagger}$, $\underline{L} = TL$, and $\underline{C} = CT^{\dagger}$. We note the use of the pseudoinverse for cases were T is not necessarily invertible. For example, to truncate modes we can use a nonsquare T matrix. For stable LTI systems there exists an invertible state transformation matrix T_{bi} such that the resulting transformed system has equal and diagonal controllability and observability Hankel singular values[20]

$$\underline{W}_c = \underline{W}_o = \text{diag}\{\sigma_1, \sigma_2, \ldots, \sigma_n\} \tag{31}$$

with Hankel singular values $\sigma_l \geq \sigma_j$ for $l < j$. The large σ values correspond to states that are well disturbed and observed. Small values of σ correspond to states that are not disturbed and/or not observed. Following model reduction arguments, these states can be removed from the model because their effect will not be seen in the measurement. Balancing ensures a proper input/output scaling. A second-state transformation matrix T_{ki} (in this case state truncation) can be formed such that $x_{bi} = T_i x = T_{ki} T_{bi} x$, where $T_{ki} = [I \;\; 0]$

is a $n_i \times n$ matrix formed with a $n_i \times n_i$ identity matrix and conformable zero matrix. This transformation extracts the first n_i states, corresponding to the n_i largest Hankel singular values.

If this model reduction is applied to the ith full-order system, we obtain $A_i = T_i A T_i^{\dagger}$, $L_i = T_i L$, and $c_i = C_i T_i^{\dagger}$ [see Eq. (20)]. Balanced reduction of the full-order local models provides a method to reduce the local models such that the disturbance to input characteristics are approximately preserved. What remains to be outlined is a tool to determine the order of the reduced-order local models.

Assuming the local models are formed using the balanced truncation, we are interested in recovering the best global state estimate from each local estimator. The local Kalman filter at each sensor node produces an estimate of the reduced and balanced state. To recover the ith estimate of the global state, we use the properties of the pseudoinverse to invert the state transformation, resulting in $x_g = T_i^{\dagger} x_{bi}$, with system matrices $A_g = T_i^{\dagger} A_i T_i$, $L_g = T_i^{\dagger} L_i$, $C_g = c_i T_i$, and $K_g = T_i^{\dagger} K_i$. Because information has been lost in the state truncation, we do not recover the global state uniquely.

B. Performance Evaluation

We develop a method to quantify the performance of the global state estimates from using the reduced-order models. The true steady-state discrete time Kalman filter follows from combining Eqs. (3) and (5), resulting in

$$\hat{x}(k+1) = A\hat{x}(k) + K[z(k+1) - CA\hat{x}(k)] \tag{32}$$

which, upon substitution of Eqs. (1) and (2), results in

$$\hat{x}(k+1) = (A - KCA)\hat{x}(k) + KCAx(k) + KCLw(k) + Kv(k+1) \tag{33}$$

The filter gain is obtained through solving the familiar algebraic discrete Riccati equation for the steady-state predict error covariance.

Similarly, the nonoptimal, decentralized filter can be written as

$$\hat{x}_g(k+1) = A_g\hat{x}_g(k) + K_g[z(k+1) - C_g A_g \hat{x}_g(k)] \tag{34}$$

where decentralized dynamics are written with a g subscript. The gain K_g is again computed by obtaining the solution of an algebraic discrete Riccati equation, where care is taken to ensure that the decentralized (from the local estimator) noise covariance is used. Substitution of the true measurement, Eq. (2), and the dynamics leads to

$$\begin{aligned}\hat{x}_g(k+1) &= A_g\hat{x}_g(k) + K_g[Cx(k+1) + n(k+1) \\ &\quad - C_g\hat{x}_g(k+1)] = (A_g - K_g C_g A_g)\hat{x}_g(k) + K_g CAx(k) \\ &\quad + K_g CLw(k) + K_g v(k+1)\end{aligned} \tag{35}$$

Generalizing the approach of Ref. 13 to discrete systems, we can determine the state estimate error for filtering with the incorrect decentralized model. Subtracting Eq. (1) from Eq. (35) results in an estimation error, given as

$$\begin{aligned}\tilde{x}(k+1) &= \hat{x}_g(k+1) - x(k+1) = (A_g - K_g C_g A_g)\tilde{x}(k) \\ &\quad + [(A_g - A) + K_g(CA - C_g A_g)]x(k) \\ &\quad + (K_g C - I)Lw(k) + K_g v(k+1)\end{aligned} \tag{36}$$

Equations (1) and (36) can be combined to form the state-space system given by

$$\begin{pmatrix}\tilde{x}(k+1)\\ x(k+1)\end{pmatrix} = \begin{pmatrix}A_g - K_g C_g A_g & (A_g - A) + K_g(CA - C_g A_g)\\ 0 & A\end{pmatrix} \times \begin{pmatrix}\tilde{x}(k)\\ x(k)\end{pmatrix} + \begin{bmatrix}(K_g C - I)U\Lambda^{\frac{1}{2}} & K_g\Theta^{\frac{1}{2}}\\ KU\Lambda^{\frac{1}{2}} & 0\end{bmatrix}\begin{pmatrix}\underline{w}(k)\\ \underline{v}(k+1)\end{pmatrix} \tag{37}$$

where the process noise and sensor noise processes have been transformed into unit-intensity white-noise processes through diagonalization of their respective covariance matrices. Equation (37) is in the form

$$q(k+1) = A_a q(k) + B_a \xi(k) \tag{38}$$

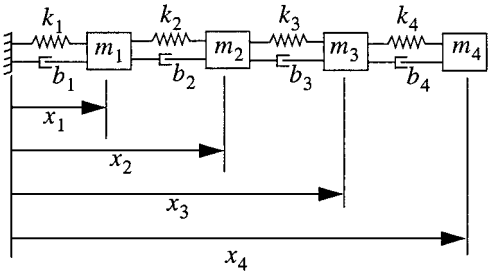

Fig. 2 Four-spring design example to demonstrate a technique for selecting reduced-order local models.

where $\xi(k)$ is a unit-intensity, white-noise process. The steady-state covariance can be found by solving the discrete-time Lyapunov equation

$$P_a = A_a P_a A_a^T + B_a B_a^T \tag{39}$$

In this case the solution is partitioned as

$$P_a = \begin{pmatrix}P_g & V^T\\ V & P_x\end{pmatrix} \tag{40}$$

where P_g corresponds to the state estimate variances of the Kalman filter with incorrect dynamics, P_x corresponds to the variance of the system state, and V corresponds to their correlation. We note that the block triangular form of A_a allows solution of the $2n \times 2n$ Lyapunov equation (39) to be computed by successively solving three $n \times n$ Lyapunov equations. However, this method requires the solution of a generalized Lyapunov equation of the form $X = AXB + C$, where $B \neq A^T$. The generalized Lyapunov equation is numerically more difficult to solve than the standard form, and thus we elect to solve Eq. (39) directly.

We can evaluate the performance of the local estimators by comparing the local state estimate error variances diag(P_g) with the global, optimal, state estimate error variances.

C. Example

A simple example will be conducted to demonstrate and explain the technique. The sample system is shown in Fig. 2. The dynamics for the system are obtained. We first write the continuous-time matrix A_c such that the homogenous dynamics are $\dot{x} = A_c x_r$, where $x = [x_1\ x_2\ x_3\ x_4\ \dot{x}_1\ \dot{x}_2\ \dot{x}_3\ \dot{x}_4]^T$. A zero-order-hold discretization of A_c is performed, resulting in a discrete A matrix. The other model elements for the example include $L = [0\ \ I]^T$ and $C = [I\ \ 0]$, where 0 is a 4×4 zero matrix and I is a 4×4 identity matrix. Thus, the four sensors directly measure the positions of the four masses, respectively. The model parameters are $\{m_1, m_2, m_3, m_4\} = \{50, 20, 6, 1\}$, $\{k_1, k_2, k_3, k_4\} = \{1, 3, 7, 10\}$, and the noise covariances are given by $\Xi = I$ and $\Theta = \mu I$.

The system is transformed into a real-modal form, with the block-diagonal dynamics matrix made up of 2×2 blocks of the form

$$A_{\text{bl}} = \begin{bmatrix}-\omega\zeta & \omega\sqrt{1-\zeta^2}\\ -\omega\sqrt{1-\zeta^2} & -\omega\zeta\end{bmatrix} \tag{41}$$

Proportional damping is chosen by assigning ζ. The modes are ordered with frequency, e.g., states 1 and 2 correspond to the first mode's states.

Figure 3 is a plot of the Hankel singular values corresponding to each full-order local model of the example of Fig. 2. We see that sensor 1 has four large singular values, which implies that four states are necessary to preserve reasonable local state estimates in the reduced-order local model. Likewise, sensor 2 requires six states, sensor 3 requires six states, and sensor 4 requires all eight states.

In Fig. 4 for the system with $\zeta = 0.001$ proportional damping, we plot the jth state's normalized accuracy

$$A_{i,j} = \frac{P(j,j)}{P_{g,i}(j,j)} \tag{42}$$

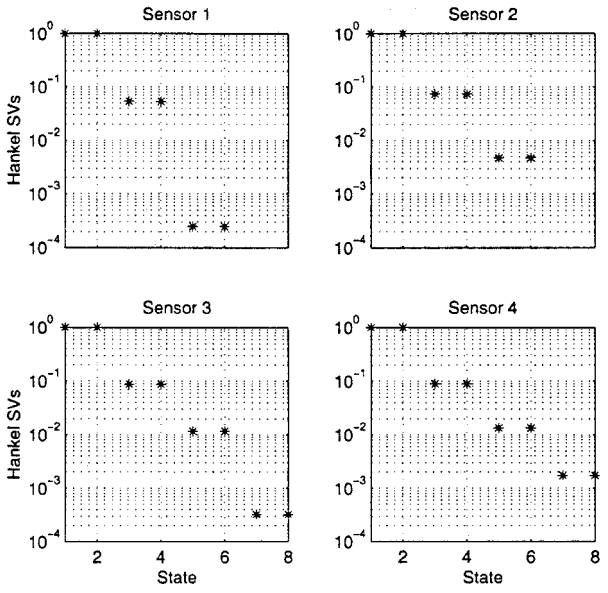

Fig. 3 Hankel singular values for balanced full-order local models corresponding to each sensor.

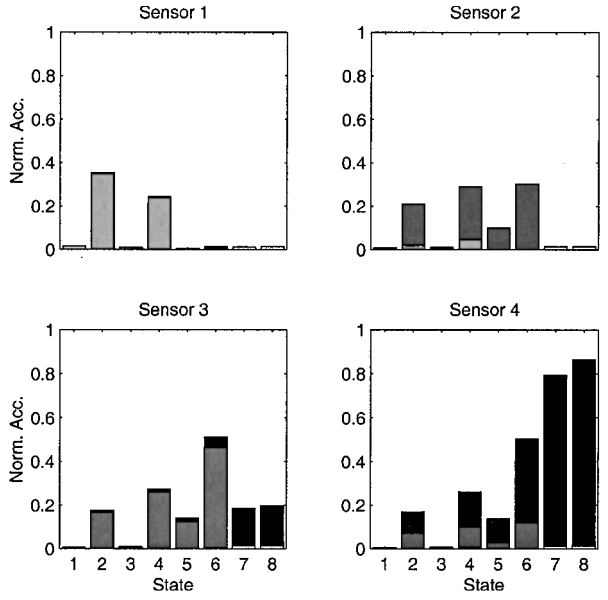

Fig. 4 Plot of normalized local estimator's global state estimate accuracies as the order of the local models is increased for proportional damping of $\zeta = 0.001$. (1 corresponds to global fully coupled estimation.) The order (2, 4, 6, 8) of the local models increases as we ascend from light to dark.

formed by the error covariance of each state's local estimator global estimate $P_{g,i}(j, j)$, normalized by the estimate error covariance of each of the states from the fully centralized, optimal Kalman filter $P(j, j)$. A value of 1 corresponds to an optimal estimate of the state. The partitions of the bar chart correspond to increasing the order of the local estimators from 2, 4, 6, to 8. The peak value of each state's estimate corresponds to the full-order local model estimate of the global state estimates corresponding to a particular sensor and provides an upper bound on the achievable performance for a local state estimator of the form required by the development of Sec. II. For example, looking at the sensor 1 chart, we see that a full-order local model can achieve an estimate for state 2, 38% as well as the centralized Kalman filter. That is, the variance of the optimal error for state 1 is 62% better than our best estimate variance from the sensor 1 local filter. (We emphasize that we are now examining local estimates of the global state, and not the optimal global estimate.) When compared with the optimal filter, the high-order local filters can only capture the states directly measured. We also note that the

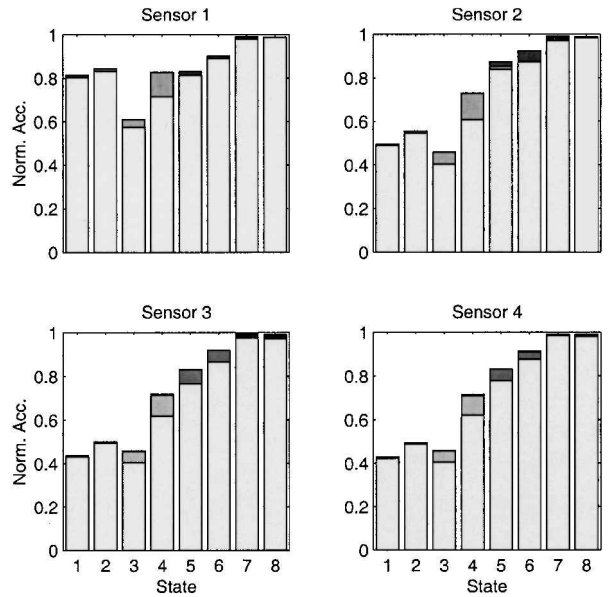

Fig. 5 Plot of normalized local estimator's global state estimate accuracies as the order of the local models is increased for proportional damping of $\zeta \rightarrow 1$. (1 corresponds to global fully coupled estimation.) The order (2, 4, 6, 8) of the local models increases as we ascend from light to dark.

high-order local estimates do not achieve the performance obtained by the global estimator. The global estimator does indeed use some information from sensors 2, 3, and 4 to estimate the position and velocity of m_1.

Figure 4 provides an engineering design tool to determine the order of the reduced-order models. A tradeoff of order and global state estimate accuracy is presented. The global estimator performs the best with an optimal normalized accuracy of 1. The derivation of Sec. II shows that a decentralized filter can be designed with one-way communication from the local nodes to recapture the optimal state estimates. In Fig. 4 the bars correspond to the cumulative accuracy of the local estimators as the local model order increases. The maximum value of the bars corresponds to the accuracy of the best possible estimates given single sensors. The loss in performance compared with the global estimators corresponds to the effect of limiting the local estimator to the use of a single sensor. The reduced-order balanced decoupled models show further performance degradation. The effect of model reduction varies from state to state. Time-series simulations validated the computed variances to within 2%.

In the case of sensor 1, we see that a point of diminishing returns is reached with a fourth-order local model such that marginal benefit is achieved by using an sixth-order model. This conclusion verifies the claim of four important singular values captured in Fig. 3. The figure also can show which states are not measured well by any sensor (e.g., state 1) and are thus estimated well only by the global filter. From examining eigenvectors we see the first mode corresponds to a motion of all four masses, which is measured equally well by all sensors, allowing the global filter to leverage averaging to minimize the effect of sensor noise. This explains the poor local estimates of states 1 and 2. As we increase in frequency, the mode shapes become more local, until the fourth mode is mainly a motion of m_4, well measured by sensor 4. However, this mode is not a dominant mode, which explains why a full eighth-order local model is required by sensor 4 to estimate states 7 and 8.

In Fig. 5 we plot the corresponding chart for the system as $\zeta \rightarrow 1$. In the case of higher damping, we see local estimates approach the global estimates with low-order local models. This is attributed to each mode having a less local (in frequency) effect, which increases the correlation between states.

IV. SIM: Detailed Design Example

The SIM is the first observatory in NASA's Origins program. What follows is the application of the developed decentralized

Table 1 SIM model sensors

Sensor	Sensor type	Measure	Plot title	Res.
1	Laser interferometer	Guide 1 DPL	DPL $g1$	10 nm
2	Laser interferometer	Guide 2 DPL	DPL $g2$	10 nm
3	Laser interferometer	Science DPL	DPL s	10 nm
4	Star tracker	x angle	θx	1 arcsec
5	Star tracker	y angle	θy	1 arcsec
6	Star tracker	z angle	θz	1 arcsec
7	Rate gyro	x angular rate	θ dot x	0.03 arcsec/s
8	Rate gyro	y angular rate	θ dot y	0.03 arcsec/s
9	Rate gyro	z angular rate	θ dot z	0.03 arcsec/s

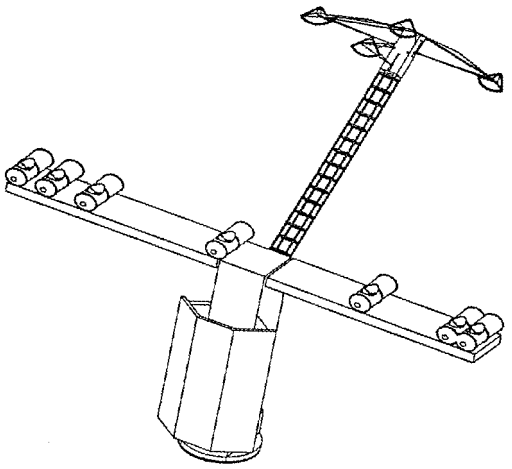

Fig. 6 One possible design of the SIM spacecraft (graphic courtesy of Jet Propulsion Laboratory.

estimation techniques to the FEM of the SIM spacecraft. The resulting analysis demonstrates the applicability of decentralization of large-scale flexible space structures. SIM is a space-based observatory designed for very-high resolution observations of astronomical targets. Figure 6 is a schematic of one possible design of the spacecraft. (In this paper the SIM model and ensuing description is for SIM Classic, an early SIM design. Current design iterations can result in a spacecraft physically quite different from this. The techniques applied to the SIM classic model are general enough to be applied to future SIM models and other large-scale systems.)

The optical side of the spacecraft is formed from a truss structure with seven collector apertures. In the standard observation mode the collectors work in pairs, with two pairs imaging bright guide stars and the third pair imaging the science target. The seventh aperture is redundant. A metrology tower rises from the truss structure. At the base of the telescope is the spacecraft bus, housing the attitude control system, communication hardware, and electronics.

The full-order FEM preserving the first 128 modes is reduced to 24 modes and discretized for use in the design example. The states are ordered such that the first six correspond to rigid-body rotational modes. A low-bandwidth attitude control system is applied to the spacecraft to slightly stiffen and to damp the rigid body modes. States 7 through 48 correspond to the first 21 structural modes of the flexible spacecraft and also account for a high-frequency dereverberated roll off. The modes are in the modal form of Eq. (41). The process noise disturbances correspond to the three 1-N rms forces (x, y, and z) and three 0.24-Nm rms torques (x, y, and z) of the reaction wheels.

The L matrix of the model is scaled such that the process noise covariance $\Xi = I$. The model sensors include laser interferometers to measure differential path length (DPL), star trackers to measure attitude angle, and rate gyroscopes to measure angular rate. The sensor suite is summarized in Table 1.

The sensor resolution gives us a measure of the sensor noise. We can choose our sensor noise variance relative to the units of the measurement output, C matrix. The laser interferometer is a very high-resolution sensor providing a measure of the structural modes of the system. The star trackers are relatively noisy sensors providing a measure of mainly the rotational modes. The rotational velocities are measured by the rate gyroscopes.

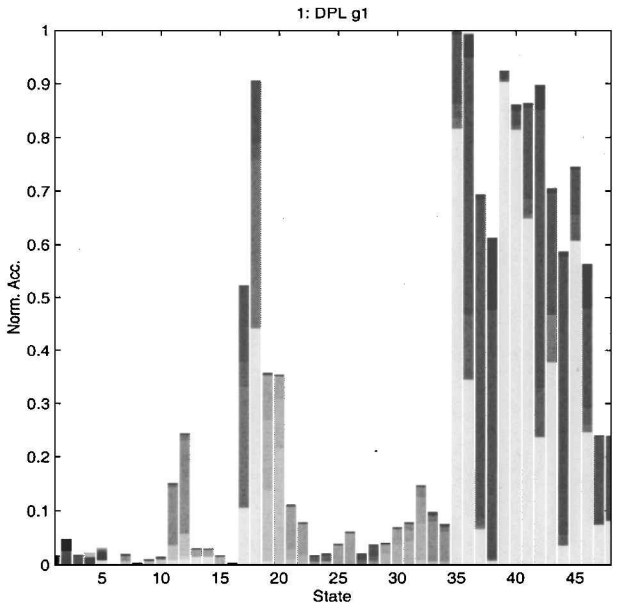

Fig. 7 Zoom of a single sensor's normalized local estimator's global state estimate accuracies as the order of the local models for SIM is increased. (1 corresponds to global fully coupled estimation.) The local order (2, 4, 8, 12, 16, 20, 24, 28, 32, 36, 40, 44, 48) is increased as we ascend from light to dark.

We are now prepared to determine the respective local models for each of the nine sensors. Figure 7 corresponds to the local state accuracy bar graph for the Guide 1 DPL as the local order is increased from 2, 4, 8, 12, 16, 20, 24, 28, 32, 36, 40, and 44 to 48. The complexity of the SIM model did require some additional work to temporarily decouple structural modes from the rotational modes. These manipulations are necessary because the low frequencies of the rotational modes are numerically troublesome for the balancing and Lyapunov solving routines (the modes numerically behave as if they are on the unit disk).

We see that states 17 and 18 are estimated well by a second-order model. This mode corresponds to a structural mode, which is strongly measured in the path length. The high-order states 36–48 are estimated well by the low-order local estimator because in this sensor they have small residues and are correlated to states 17 and 18. Increasing the order of the local model allows a voice coil mode (states 11 and 12) directly in the DPL to be estimated. This figure gives us an idea of the global states that are well estimated by the local model and allows us to compare to the accuracy achieved by the global estimator. With knowledge of the importance of specific states on the performance and requirements on state estimation accuracy (for identification or control), we can evaluate the sensors one at a time.

Figure 8 is a state bar graph for SIM showing the normalized global state estimation errors made by all nine local estimators as their orders are increased from 8, 16, 32, to 48. Again the performance of the global estimates made by the local estimators improves as the order of the local estimators is increased. Local estimation cannot achieve good (relative to the global estimator) state estimates for states 20–36. Thus, no single sensor provides a good measure of these states, and sensor fusion is required to estimate them. This supports the notion that a system like SIM has some modes that cannot be well estimated without fusing data from multiple sensors. The rotational rigid-body states (1–6) are estimated better with the rate gyroscopes because they are modeled with lower noise than the star trackers.

By studying the marginal improvement in local estimates as the local order is increased, the following orders are selected for the reduced-order models: 18 for laser interferometer sensors, 2 for star trackers, and 24 for rate gyroscopes. Figure 9 plots the singular values from the six disturbances to the sensor output as a function

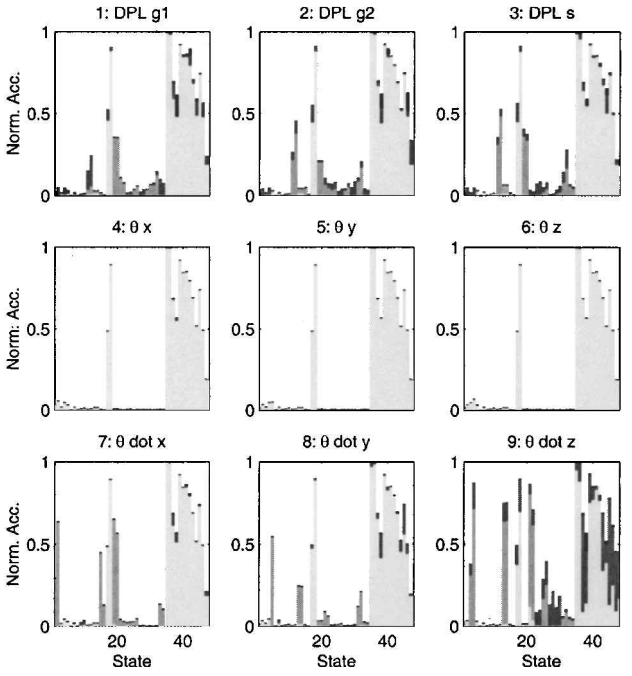

Fig. 8 Plot of normalized local estimator's global state estimate accuracies as the order of the local models for SIM is increased. (1 corresponds to global fully coupled estimation.) The local order (8, 16, 32, 48) is increased as we ascend from light to dark. (For presentation purposes only four local model orders are used.)

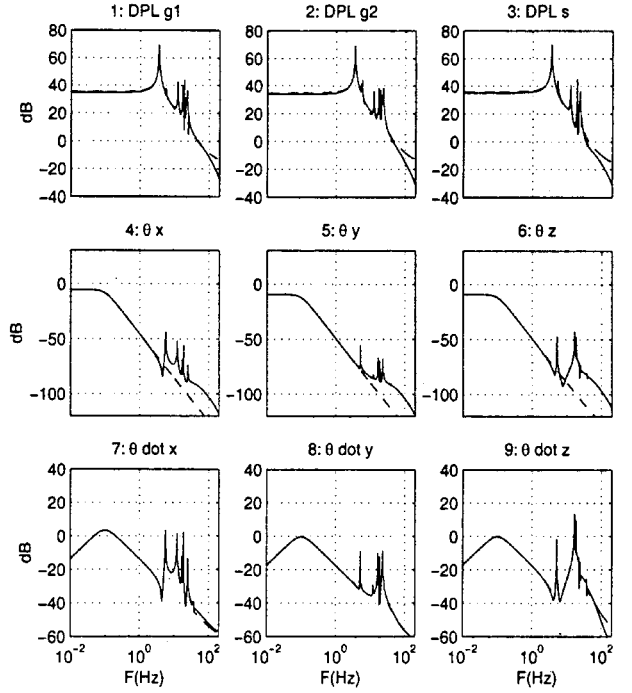

Fig. 9 Singular values from disturbance to each sensor of the SIM model. ——, corresponds to full-order local models, and - - -, corresponds to reduced-order local model.

of frequency. This plot provides a measure of the levels of response given white-noise process noise and provides a feel for the spectral content of the sensor measurements. The laser interferometer sensors contain good measures of the structural response, but a poor measure of the low-frequency rotational modes. The star trackers provide a very strong measure of the low-frequency rotational mode, which swamps information from the structural modes. This explains why the star tracker sensor only obtains a marginal increase in estimate performance as the reduced-order model increases beyond order 2. The rate gyroscope sensors provide a measure of the derivative of the rotational modes, but at the same time preserves a reasonable measure of the structural modes. We conclude that the accuracy of a local estimate depends on the sensor observability (how states are observed) and on the sensor quality (sensor noise).

Local models for estimation have been deduced for the SIM spacecraft. Some system states are estimated well by the local models. If these are states relevant for local control, we conclude that local control can perform well. Some states are not estimated well by the local models, and if these inaccurately estimated states are excited by a local control design, instability or poor performance can result. The local estimates have been designed within the framework of Sec. II so that these estimates can be combined to recover the optimal global estimate if desired.

V. Conclusion

A decentralized estimator that preserves the optimal global estimates has been detailed. The estimator combines local estimates made at each sensor node to recover the optimal estimates. A technique based on model reduction theory is introduced for determining the local models. In addition, a technique to determine the best global state estimates from linear combinations of a local mode is derived.

A detailed design example is performed by decentralizing the state estimation problem for the SIM spacecraft. Some states are found to be estimated very well by reduced-order local estimators, whereas others are estimated well only by fusing information from all sensors. We conclude that SIM is not a good candidate model for local state estimation. Future work includes a dual study to determine the suitability of SIM for local control. This work has established the advantage of global estimation for estimating the state of the spacecraft. The developed local state fusion can combine the local estimates to recover the optimal state estimate.

Appendix: Optimal Information Filter

The information filter is an alternate form of the Kalman filter.[9,12,21] It is algebraically equivalent to the Kalman filter, producing the optimal state estimate and covariance matrix at each time step. More accurately, an information matrix is generated at each step and is defined by the relation

$$Y(i \mid j) \equiv P^{-1}(i \mid j) \tag{A1}$$

where $P(i \mid j)$ is the ith error covariance, given the jth measurement. This information matrix has the property that when it is large it implies that we have much information about the state and that the state estimate is good. The information state is defined from the system state with the transformation

$$y(i \mid j) \equiv Y(i \mid j)x(i \mid j) \tag{A2}$$

Consider the model given by Eqs. (1) and (2). The discrete Kalman filter is given in Eqs. (3–7). We begin the derivation by defining the invertible term $S = CP_mC + \Theta$ and rewriting a term of Eq. (6) as

$$I - KC = (I - KC)P_mP_m^{-1} = \left(P_m - KSS^{-1}CP_m\right)P_m^{-1} \tag{A3}$$

where for simplicity the index dependence has been suppressed and the definition of P and P_m from Sec. II has been employed. Now, we substitute Eq. (7) for K to write

$$I - KC = \left(P_m - P_mC^TS^{-1}CP_m\right)P_m^{-1} = PP_m^{-1} \tag{A4}$$

Rewriting Eq. (5) and substituting Eq. (7) results in

$$\hat{x}(k+1) = (I - KC)\hat{x}(k+1 \mid k) + Kz(k+1)$$

$$= PP_m^{-1}\hat{x}(k+1 \mid k) + Kz(k+1) \tag{A5}$$

By multiplying by P^{-1} and substituting Eq. (7) for K, we can rewrite in terms of information variables as

$$\hat{y}(k+1) = \hat{y}(k+1 \mid k) + C^T\Theta^{-1}z(k+1) \tag{A6}$$

By applying the Matrix Inversion Lemma to Eq. (6), we can write

$$P^{-1}(k+1) = P_m^{-1} + C^T\Theta^{-1}C \tag{A7}$$

By substituting the information definitions into Eqs. (3) and (4), we can write the predict cycle for the information filter as given by Eqs. (8) and (9). The update cycle can be deduced from Eqs. (48) and (49).

Acknowledgment

The SIM Classic model was provided to the Massachusetts Institute of Techology (MIT) Space Systems Lab by the Jet Propulsion Laboratory for contract SIM: 961-123, with technical monitor Sanjay Joshi. The authors are grateful for the suggestions and comments provided by Joshi. The manuscript benefitted from the suggestions of the anonymous reviewers and of Scott Uebelhart of the MIT Space Systems Laboratory. The first author acknowledges the suggestions of M. Athans of the MIT Laboratory for Information and Decision Systems.

References

[1]Neat, G. W., Abramovici, A., Melody, J. W., Calvet, R. J., Nerheim, N. M., and O'Brien, J. F., "Control Technology Readiness for Spaceborne Optical Interferometer Missions," The Space Microdynamics and Accurate Control Symposium, May 1997.

[2]Mallory, G. J. W., and Miller, D. W., "SIM Control: Controlled Structures Approach," Internal Document, Jet Propulsion Lab., California Inst. of Technology, March 1998.

[3]Siljak, D. D., *Large-Scale Dynamic Systems, Stability and Structure*, North-Holland, New York, 1978, pp. 192–199.

[4]Sandell, N. R., Jr., Varaiya, P., Athans, M., and Safonov, M. G., "Survey of Decentralized Control Methods for Large Scale Systems," *IEEE Transactions on Automatic Control*, Vol. AC-23, No. 2, 1978, pp. 108–128.

[5]Sundareshan, M. K., and Elbanna, R. M., "Design of Decentralized Observation Schemes for Large-Scale Interconnected Systems: Some New Results," *Automatica*, Vol. 26, No. 4, 1990, pp. 789–796.

[6]Saif, M., and Guan, Y., "Decentralized State Estimation in Large-Scale Interconnected Dynamical Systems," *Automatica*, Vol. 28, No. 1, 1992, pp. 215–219.

[7]Speyer, J. L., "Computation and Transmission Requirements for a Decentralized Linear-Quadratic-Gaussian Control Problem," *IEEE Transactions on Automatic Control*, Vol. AC-24, No. 2, 1979, pp. 266–269.

[8]Willsky, A. S., Bello, M. G., Castanon, D. A., Levy, B. C., and Verghese, G. C., "Combining and Updating of Local Estimates and Regional Maps Along Sets of One-Dimensional Tracks," *IEEE Transactions on Automatic Control*, Vol. AC-27, No. 4, 1982, pp. 799–813.

[9]Manyika, J., and Durrant-Whyte, H., *Data Fusion and Sensor Management, a Decentralized Information Theoretic Approach*, Ellis Horwood, New York, 1994, pp. 1–269.

[10]Mutambara, A. G. O., *Decentralized Estimation and Control for Multisensor Systems*, CRC Press, Boca Raton, FL, 1998, pp. 1–230.

[11]Hashemipour, H. R., Roy, S., and Laub, A. J., "Decentralized Structures for Parallel Kalman Filtering," *IEEE Transactions on Automatic Control*, Vol. AC-33, No. 1, 1988, pp. 88–94.

[12]Roy, S., Hashemi, H. R., and Laub, A. J., "Square Root Parallel Kalman Filtering Using Reduced-Order Local Filters," *IEEE Transactions on Aerospace and Electronic Systems*, Vol. 27, No. 2, 1991, pp. 276–289.

[13]Gelb, A. (ed.), *Applied Optimal Estimation*, Massachusetts Inst. of Technology Press, Cambridge, MA, 1974, pp. 229–276.

[14]Roy, S., and Iltis, R. A., "Decentralized Linear Estimation in Correlated Measurement Noise," *IEEE Transactions on Aerospace and Electronic Systems*, Vol. 27, No. 6, 1991, pp. 939–941.

[15]Penrose, R., "A Generalized Inverse for Matrices," *Proceedings of the Cambridge Philosophical Society*, Vol. 51, 1955, pp. 403–496.

[16]Bierman, G. J., "A Comparison of Discrete Linear Filtering Algorithms," *IEEE Transactions on Aerospace and Electronic Systems*, Vol. 9, No. 1, 1972, pp. 28–37.

[17]Kerr, T. H., "Decentralized Filtering and Redundancy Management," *IEEE Transactions on Aerospace and Electronic Systems*, Vol. 23, 1987, pp. 83–119.

[18]Sezer, M. E., and Siljak, D. D., "Nested ε-Decompositions and Clustering of Complex Systems," *Automatica*, Vol. 22, No. 3, 1986, pp. 321–331.

[19]Finney, J. D., and Heck, B. S., "Matrix Scaling for Large-Scale System Decomposition," *Proceedings of the American Control Conference*, AACC, Seattle, WA, 1995, pp. 2918–2923.

[20]Zhou, K., Doyle, J. C., and Glover, K., *Robust and Optimal Control*, Prentice–Hall, Upper Saddle River, NJ, 1996, pp. 155–171.

[21]Willsky A., "Recursive Estimation, Supplementary Notes," Dept. of Electrical Engineering and Computing Science, Massachusetts Inst. of Technology, Cambridge, MA, 1994.